Theoretical Study of the Oxidation Mechanism of Aromatic Amines

Daniel Larumbe,[a] Miquel Moreno,[a] Iluminada Gallardo,[a] Juan Bertrán[a] and Claude P. Andrieux[b]

[a] *Departament de Química, Universitat Autònoma de Barcelona, 08193 Bellaterra, Catalonia, Spain*
[b] *Laboratoire d'Electrochimie Moléculaire, Université Paris 7, 2 Place Jussieu, 75251 Paris Cedex 05, France*

The overall mechanism of the chemical step involved in the electrochemical oxidation of tertiary aromatic amines has been investigated by means of the quantum-chemical AM1 method. By using the parent compound aniline as a model it is found that, in good accord with previous electrochemical data, dimerization of two radical cations takes place before deprotonation, the dimerization step involving a higher energy barrier.

An analysis of the radical cations of different aromatic amines shows that the unpaired electron is mainly located at the carbon in the *para* position with respect to the amino group. This resonant effect is reduced when more than one aromatic ring is attached to the nitrogen so that triphenylamine is much less reactive than *N,N*-dimethylaniline.

Finally, the observed lack of reactivity of *para*-substituted carbons is attributed to the inability of leaving groups to form stable cations.

Deprotonation at carbon is a commonly proposed reaction for many organic cation radical intermediates. For example, this is the generally accepted reactivity of alkylaromatic and tertiary amine cation radicals generated in chemical,[1] electrochemical[2] and photochemical[3] oxidation reactions. In spite of their importance, these proton-transfer reactions have not received much attention and are, therefore, poorly understood as compared with the proton-transfer reactions from even-electron molecules.

Several electrochemical studies have dealt with the oxidation of aromatic amines. These studies have shown that tertiary aromatic amines bearing substituents in the phenylic *para* position form stable radical cations.[4–8] However, for aromatic amines without *para* substitution the radical cation is not stable but leads to a benzidine after dimerization and loss of two protons.[9] The global mechanism can be written as shown in eqns. (1) and (2).

$$C_6H_5N< - e^- \longleftrightarrow C_6H_5N<^{\bullet+} \quad (1)$$

$$2(C_6H_5N<^{\bullet+}) \longrightarrow >N\text{–}C_6H_4\text{–}C_6H_4\text{–}N< + 2H^+ \quad (2)$$

The overall mechanism of the chemical step (2) has recently been investigated by means of electrochemical methods[10,11] for triphenylamine and *N,N*-dimethylaniline showing that, in spite of the previous data, the process of deprotonation occurs after dimerization between two radicals has taken place. Moreover, it is seen that the whole process follows second-order kinetics so that the rate-determining step is bimolecular.

From a theoretical point of view only the structure of the aniline molecule and some other aromatic amines have been studied, mainly by means of semiempirical techniques.[12–18] However, to our knowledge no work has been devoted up to now on a study of radical cations and the oxidation mechanism of aromatic amines. In this paper we present such a study in order to clarify the mechanism of the chemical process (2) and to comprehend from a theoretical point of view the factors that govern the electrochemical data. The parent compound, aniline, is chosen in order to facilitate full calculations of the different steps involved in the reaction. Some calculations are also performed for other aromatic amines such as *N,N*-dimethylaniline and triphenylamine, the two compounds previously studied by means of electrochemical techniques. A *para*-substituted aromatic amine, *p*-bromoaniline, is also considered in order to understand why the oxidative process is inhibited with *para* substitution.

Method

Owing to the size of the molecules we deal with, a semiempirical method is required. In particular, we have chosen the recent AM1 method of Dewar *et al.*[19] which overcomes most of the weaknesses of the previous MNDO model.[20] The AM1 method is known to provide reliable results for aromatic compounds.[21–23] Recently, the AM1 method has also been successfully used to analyse bond-dissociation energies of radical cations.[24]

The unrestricted Hartree–Fock method (UHF) is used for closed- and open-shell systems.[25] UHF methodology is known to give satisfactory results when dealing with radical structures.[26–28] The drawback of spin contamination which may take place mainly when dealing with singlet structures, does not appreciably affect our calculations as contaminations are below the 10% mark[29] with one exception that will be discussed in the next section.

The equilibrium geometries of all the molecules were fully optimized using the Davidon–Fletcher–Powell conjugated gradient algorithm.[30] All the geometry optimizations were performed without any assumption of symmetry being imposed. Kinetics of elementary processes were studied within the reaction-coordinate procedure. That is, taking one (or two) geometric parameters as the reaction-coordinate-independent variables we optimized the rest of the geometry at a given set of values. A direct location of transition states was also carried out through minimization of the square of the gradient norm.[31] Numerical evaluation and diagonalization of the force-constant matrix was also undertaken in order to ensure that transition states had only one negative eigenvalue.

All the calculations were performed using MOPAC[32] and AMPAC[33] programs.

Results and Discussion

We begin this section with the kinetic analysis of the

dimerization process for the aniline. In fact, owing to the presence of N–H bonds, the oxidation of aniline would lead to an azobenzene or to a precursor of a quinone diimide.[34] However, from a theoretical point of view we can disregard the reactivity of the N–H bonds and focus interest on the C–H bond cleavage so that a mechanism leading to benzidine is studied. This way we expect that the reactivity of aniline, as a model, will be similar to that of the experimentally studied *N,N*-dimethylaniline. This point will be assessed later on.

Afterwards, we analyse the geometries and electronic characteristics of the intermediates involved in the entire reaction. A comparison with different aromatic amines is also given in order to identify the differences and study how these affect the reactivity in the oxidative pattern.

Oxidative Dimerization of Aniline.—Once the radical cation has been formed, dimerization and deprotonation must occur so that the experimental product is finally obtained. However, it is not *a priori* known whether dimerization precedes loss of a proton or *vice versa*. In other words, two different mechanisms are consistent with the electrochemical data.

As the cleavage of a C–H bond was very difficult to achieve owing to problems with the SCF convergence during the reaction coordinate calculations, a water molecule solvating each of the leaving hydrogens was added in all the calculations performed in this subsection. These waters also represent a crude model of the solvent acting as proton acceptor. Note that this water molecule is not located at its preferred position (which would be with the water oxygen solvating one of the hydrogens bonded to the nitrogen) but it is used in order to lower the energy of the leaving proton.

This way, a hydronium H_3O^+ molecule is obtained instead of a proton. The AM1 method is known to be specially suited to describe intermolecular hydrogen bonds.[35–37]

Fig. 1 shows schematically the energy of the initial, intermediate and final states and the reaction paths connecting them for the two mechanisms above proposed. Note that steps (*a*) and (*b*) form mechanism 3 (dimerization preceding deprotonation) whereas steps (*c*) and (*d*) are part of mechanism 4 (deprotonation preceding dimerization). On the other hand, Fig. 2 presents the actual geometries of all the stationary points located. Structures **I**–**IV** in Figs. 1 and 2 refer to the energetic minima shown in mechanisms 3 and 4 whereas TS1 and TS2 refer to transition-state geometries.

At first glance, Fig. 1 clearly shows that from energy considerations mechanism 4 is highly unfavoured. That is, the intermediate radical is much less stable than the dicationic dimer so one is compelled to conclude that the true mechanism follows mechanism 3.

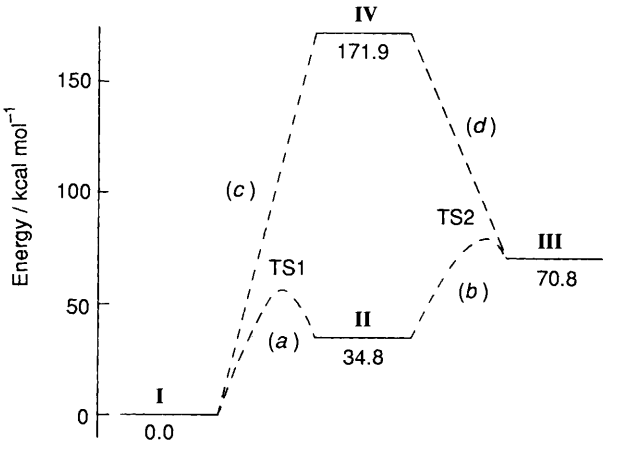

Fig. 1 Energetic scheme for the oxidative dimerization of aniline. Structures **I** and **III** refer to reactant and product, respectively, whereas **II** and **IV** are the intermediates. Dashed lines show the reaction paths of mechanisms 3 and 4. Note that steps (*a*) and (*b*) belong to mechanism 3, whereas (*c*) and (*d*) belong to mechanism 4. Geometries of structures **I**–**IV** as well as the two transition states located (TS1 and TS2) are presented in Fig. 2.

However, this simple thermodynamic study of reactants, products and intermediates without further kinetic considerations may lead to incorrect conclusions regarding the actual mechanism of the reaction. For instance, we do not know whether the dicationic dimer is a true precursor of the final product. Therefore, in order to affirm that mechanism 3 is taking place, we must convince ourselves that reactions (*a*) and (*b*) are feasible and that they do not imply too high an energy barrier.

In order to analyse this point fully, a reaction coordinate study has been performed for the different elementary mechanisms involved in the above-mentioned mechanisms 3 and 4. First we will consider the, *a priori*, less favoured mechanism 4. Step (*d*) implies dimerization of two radicals and therefore does not present any interesting feature as it is well known that the encounter of two radicals will result in direct dimerization with no energy barrier.

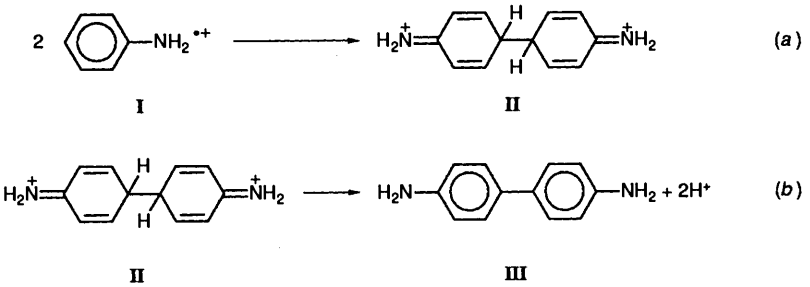

Mechanism 3

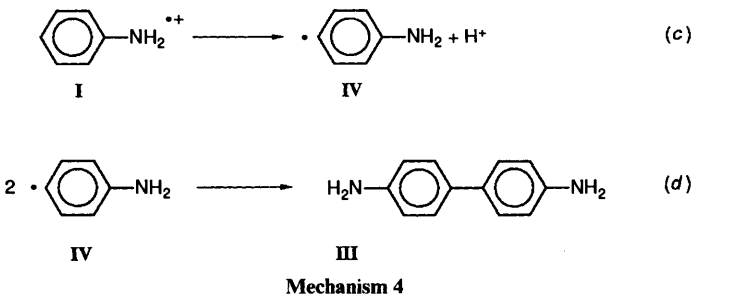

Mechanism 4

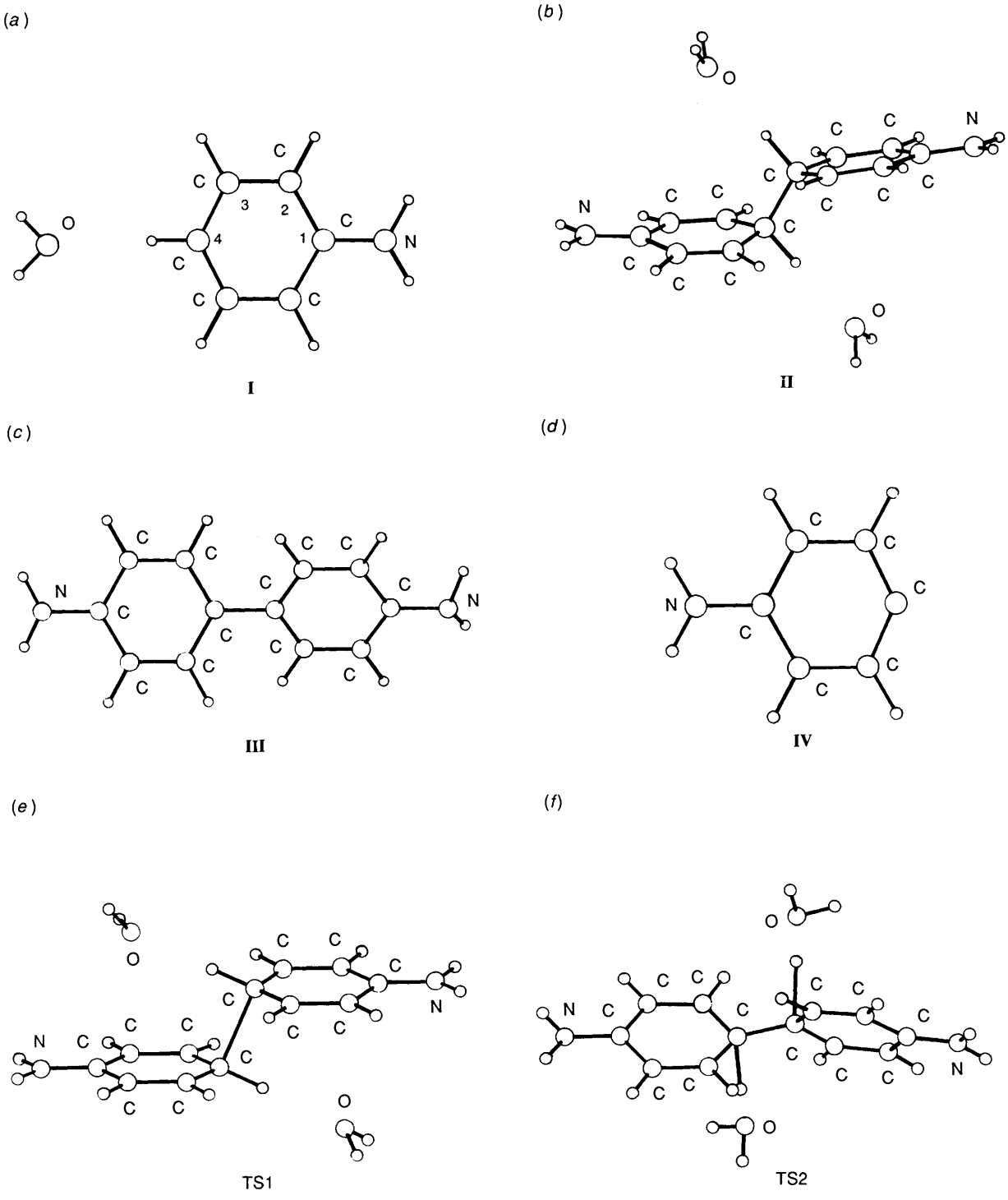

Fig. 2 Geometries of the stationary points located for the oxidative dimerization of aniline (see Fig. 1)

Of more interest is the first step of mechanism (*c*) which involves the extraction of a proton from the radical cation. This process has been followed by considering the C–H bond distance as the obvious reaction coordinate parameter. Calculations show that the energy increases monotonically from the radical until it has lost a hydronium molecule. Additional confirmation that no minima exist along the reaction path is obtained from the fact that by taking the radical and the hydronium molecules at large distances and by fully optimizing the geometry, the proton is transferred so that the structure of reactant **I** is reached.

An analysis of the orbitals along the reaction coordinate reveals that the unpaired electron that lies in a π-type orbital in the radical cation switches to a σ-type orbital when the C–H distance increases above 2.0 Å. This fact clearly establishes a link between the oxidative C–H bond cleavage and the reduction of haloaromatic compounds where a π–σ electronic transference was also observed in the C–X bond breaking process.[38]

Let us now consider the two steps involved in mechanism 3. Step (*a*), which involves dimerization of two radical cations, has been studied in reverse (*i.e.*, instead of the formation of the dimer, its breakdown has been considered). The C–C bond distance between the rings has been used as a reaction coordinate to obtain an energy profile that presents a maximum located at an energy 60.5 kcal mol^{-1} above the reactants (two radical cation molecules).

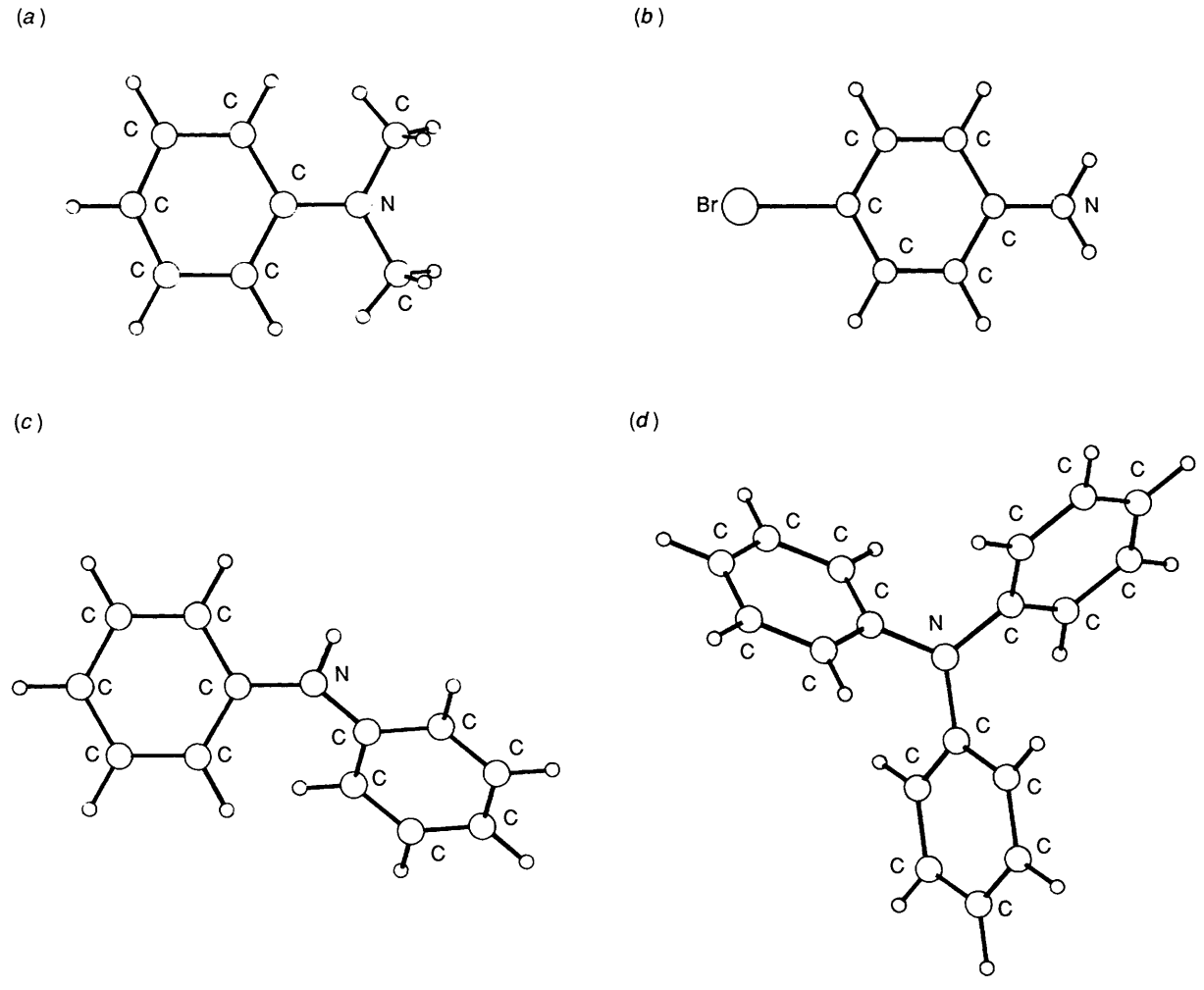

Fig. 3 Geometries of radical cations for some aromatic amines: (*a*) *N*,*N*-dimethylaniline, (*b*) *p*-bromoaniline, (*c*) diphenylamine, (*d*) triphenylamine

By using the structure of the maximum as a starting point, a direct location lead to a stationary point whose geometry is also shown in Fig. 2 (TS1). Analysis of the second derivatives of the energy showed only one negative eigenvalue. The corresponding eigenvector was related mainly to the formation of the C–C bond between the rings. By comparing this structure with the dicationic dimer (**II** in Fig. 2) it is also clear that only this C–C distance has increased. Thus, it seems that TS1 is the true transition state for step (*a*). The energy barrier is then 59.3 kcal mol^{-1} for the dimerization process and 24.5 kcal mol^{-1} for the reverse reaction. Therefore, step (*a*) represents a feasible and reversible elementary step. Note, however, that as step (*a*) has been studied in reverse, it departs from a singlet structure **II** and leads to two doublets (structure **I**). In this manner, the reaction coordinate shows an important level of spin contamination. In fact, $<S^2>$ is 1.16 at the transition state (TS1) structure so that the 'true' transition-state energy would be somewhat higher than the value found here.

Deprotonation of the dimer [step (*b*) in mechanism 3] is not so straightforward to study as now two C–H bonds are breaking a bidimensional reaction coordinate definition would be required. However, we performed a monodimensional calculation by supposing that the two C–H bond lengths remain equal, so that a synchronous bond breaking occurs. The maximum-energy structure located in this way was again used to perform a direct localization that lead to a structure where both C–H bond breaking distances remained almost equal. This geometry, TS2 in Fig. 2, again had only one negative eigenvalue of the force-constant matrix, indicating that it is a transition state. The transition vector of this structure, which is located 43.4 kcal mol^{-1} above the reactants (structure **II**), indicates the synchronous breaking of the two C–H bonds, whereas the two new O–H bonds strengthen. Although an asynchronous or two-step C–H bond breaking may present a lower-energy saddle point, the energy barrier along this synchronous mechanism route clearly provides an upper bound to the energy barrier of this process.

In conclusion, theoretical analysis has confirmed that mechanism 3, *i.e.* dimerization preceding deprotonation, is kinetically favoured. This result is in good accord with the electrochemical data for aromatic amines. Further agreement is obtained when comparing the energy barriers of process (*a*) -59.3 kcal mol^{-1} with those of (*b*) and the reverse (*a*) step which are 43.4 and 24.5 kcal mol^{-1}, respectively (see Fig. 1). Under these conditions the steady-state approximation will hold for the intermediate dimer concentration and second-order kinetics will be followed. Note that this result is unaffected by the fact that the first barrier may be too low owing to spin contamination, whereas the second one may be too high because an asynchronous mechanism has not been considered.

Electronic Structure of Intermediates.—As the dimerization of the radical cation is the rate-determining step of this process our interest is now focused on the analysis of radical cations and their corresponding dicationic dimers.

In Fig. 3 the structures of the radical cations we have studied are given. Figs. 3(*a*) and (*b*) show the structures of two mono-aromatic amines *N*,*N*-dimethylaniline and *p*-bromoaniline,

respectively, and Figs. 3(*c*) and (*d*) give the structures of the radical cations of diphenyl and triphenyl amine, respectively.

Let us first analyse the electronic structure of monoaromatic amines in order to comprehend the dimerization process. To this aim Table 1 lists the coefficients of the highest-occupied α molecular orbital, α-HOMO (which in some senses is the unrestricted Hartree–Fock equivalent of the semioccupied molecular orbital, SOMO, of a simpler restricted Hartree–Fock calculation).

This orbital, which is of π-type, is delocalized along the aromatic rings and the nitrogen atom. However, by looking at the values given in the first row of Table 1 (corresponding to aniline) it is clear that the atoms have different degrees of participation in this orbital, the more important clearly coming from C(4), *i.e.*, the carbon located *para* with respect to the amino group [see Fig. 2(*a*)]. In other words, the radical cation is mainly represented by the resonant structure **R**. Geometric

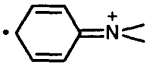

R

analysis of bond distances between aromatic carbons confirms this point. These values are given in Table 2. We see that the C(2)–C(3) distance is the shortest, therefore a stronger bond exists between those carbons. This result clearly supports the suggestion that **R** makes a large contribution to the resonance hybrid.

If the preceding analysis is true we must expect that the dimerization process will take place mainly in the *para* position. From experiment, it is known that only the *para* disubstituted dimer is obtained.[11] From a theoretical point of view, we have also not been able to obtain an *ortho* or *meta* dicationic dimer for the aniline case. We also expect that the aromatic character of the phenylic ring, partially broken down in the radical cation, will disappear in the dimer so that the double-bond character between C(2) and C(3) will be enforced.

The geometry of the dicationic dimer also shown in Fig. 2(*b*) and Table 2 for aniline confirms these predictions, the C(1)–C(2), C(2)–C(3) and C(3)–C(4) distances being 1.46, 1.35 and 1.49 Å, respectively. Note that as the two *para* carbon atoms that bond together in the dimer do not have any double-bond character they exhibit the tetrahedral bond pattern characteristic of sp^3 hybridization so that the dicationic molecule is not planar. In contrast, the final product (**III**) which results from loss of two protons from the dicationic dimer has both aromatic rings almost in the same plane, as now there is π-conjugation between the aromatic rings. This confirms that the dimerization takes place only in the *para* position. This structure is also shown in Fig. 2(*c*) and Table 2. Note that TS1, the transition state between **I** and **II**, has an intermediate geometry between the two minima. The same is true for TS2, the transition state between **II** and **III**.

Very similar trends to those observed for aniline can be readily seen in Tables 1 and 3 and Fig. 3 for *N,N*-dimethylaniline and *p*-bromoaniline. Thus we expect that the dimerization of these two species will not be appreciably different from the aniline case. This is confirmed by calculating the structures of the dicationic dimers of these two species. Energies relative to the radical cation are also very similar so that the oxidation process of *N,N*-dimethylaniline is expected to be analogous to that found for aniline.

p-Bromoaniline also forms an initial dicationic dimer. However, its further evolution to the final neutral product is not expected to take place since it would involve the cleavage of a C–Br bond leading to the formation of a bromine cation, a process that must be highly unfavoured. Thus, it seems that the experimental observation that the *para*-substituted aromatic amines do not undergo oxidation is not a result of the inability of these compounds to form dicationic dimers but rather of the fact that subsequent bond cleavage is not feasible, at least when the leaving group does not form a stable cation.

Finally, we will consider the two polyaromatic amines, diphenylamine and triphenylamine. Geometries of the radical cations are shown in Fig. 3 [(*c*) and (*d*)] and the main geometrical parameters are listed in Table 3. Compared with the aniline case, bond distances between the aromatic ring carbons differ only slightly, so it seems that the resonant form **R** which locates the radical character on the *para* carbon atom, is now of less importance.

Further insight regarding this point is obtained by analysing the α-HOMO coefficients given in the two last rows of Table 1. Comparing these values for each of the anilines, it is clear that the *para* carbon atom is always the one with the largest coefficient, but its value clearly diminishes with increasing number of aromatic rings (0.63 in aniline, 0.28 in triphenylamine). In fact, this decrease does not take place only at the carbon in the *para* position but at all the ring carbon atoms. On the other hand, the coefficient on the nitrogen only suffers a small diminution so that in triphenylamine it almost equals the coefficient of the *para* carbon atom.

These results seem to indicate that now the whole resonant effect is delocalized between two or three *para* carbons. Thus the α-HOMO coefficients of the *para* carbons on triphenylamine, diphenylamine and aniline follow approximately a linear progression 0.2:0.4:0.6. This 'dilution' effect of the radical character allows us to explain why it has been found experimentally that triphenylamine is much less reactive than *N,N*-dimethylaniline.

Note that this delocalization effect is not affected by the lack of coplanarity between aromatic rings which occurs in

Table 1 α-HOMO coefficients for some aromatic amines

Radical cation	N	C(1)	C(2)	C(3)	C(4)
Aniline	−0.38	0.37	0.36	−0.17	−0.63
N,N-Dimethylaniline	−0.38	0.35	0.35	−0.18	−0.62
p-Bromoaniline	−0.27	0.28	0.25	−0.18	−0.54
Diphenylamine	−0.29	0.25	0.22	−0.14	−0.48
Triphenylamine	−0.27	0.15	0.11	−0.07	−0.28

Table 2 Main geometrical parameters for the species involved in the oxidative dimerization of aniline

Species[a]	N–C(1)[b]	C(1)–C(2)[b]	C(2)–C(3)[b]	C(3)–C(4)[b]	N–H[b]	C(2)–H[b]	C(3)–H[b]	C(4)–H[b]	C(4)–C(4′)[b,c]	φ(C,C′)[c,d]	φ(NR$_3$)[e]
I	1.34	1.45	1.38	1.41	1.00	1.10	1.10	1.11	—	—	0
II	1.33	1.46	1.35	1.49	1.00	1.11	1.11	1.15	1.54	10.7	1.9
III	1.41	1.42	1.39	1.40	1.00	1.10	1.10	—	1.46	36.8	51.5
IV	1.38	1.43	1.40	1.37	0.90	1.10	1.10	—	—	—	0
TS1	1.33	1.46	1.36	1.44	1.00	1.11	1.11	1.11	2.06	3.5	0.9
TS2	1.35	1.43	1.37	1.43	1.00	1.10	1.11	1.61	1.48	55.9	5.3

[a] For numeration see Fig. 1. [b] Distance in Å. [c] Primes refer to the second ring when present. [d] Dihedral angle between two aromatic rings in degrees. [e] Dihedral angle between the NR$_3$ substituents in degrees.

Table 3 Main geometrical parameters for the radical cations of some aromatic amines

Species[a]	N–C(1)[b]	C(1)–C(2)[b]	C(2)–C(3)[b]	C(3)–C(4)[b]	N–H[b]	C(2)–H[b]	C(3)–H[b]	C(4)–H[b]	φ(C,C')[c,d]	φ(NR_3)[e]
N,N-Dimethylaniline	1.36	1.44	1.38	1.41	1.45	1.10	1.10	1.10	—	0
p-Bromoaniline	1.34	1.45	1.38	1.42	1.00	1.10	1.11	1.84[f]	—	0
Diphenylamine	1.40	1.43	1.41	1.42	1.02	1.09	1.09	1.09	47.8	0.5
Triphenylamine	1.43	1.44	1.41	1.42	—	1.09	1.09	1.09	74.9	0.8

[a] For numeration see Fig. 1. [b] Distance in Å. [c] Primes refer to the second ring when present. [d] Dihedral angle between two aromatic rings in degrees. [e] Dihedral angle between the NR_3 substituents in degrees. [f] C–Br distance.

polyaromatic amines for steric reasons. As detailed in Table 3 we realize that in triphenylamine the phenyl rings are twisted 74.9° whereas a more moderate value is obtained for diphenylamine. On the other hand, Tables 2 and 3 also show that the three bonds of nitrogen remain almost coplanar for all the radical cations studied. Thus, the preservation of an sp^2 bond pattern for the nitrogen seems to be the most important factor in guaranteeing a maximum degree of overlap between the nitrogen p orbital and the aromatic π orbitals.

Conclusions

An analysis of the different intermediates involved in the oxidation of aromatic amines, as well as reaction coordinate calculations, has shown that the chemical process follows mechanism 3, *i.e.*, dimerization precedes deprotonation. In accordance with the experimental results, the rate-determinating step is found to be bimolecular.

An analysis of bond distances and of the coefficients of the α-HOMO orbital of the radical cations has indicated that the resonant structure with the unpaired electron in the carbon atom situated *para* with respect to the amino group has an important weight and, thus, the aromaticity of the ring is partially broken. This effect is reduced when more than one phenylic group is attached to the nitrogen so that triphenylamine is less reactive than *N,N*-dimethylaniline, again in good accord with experimental data.

It has been found that *p*-bromoaniline does form the dicationic dimer. The experimentally observed lack of reactivity of these *para*-substituted compounds may be attributed to the inability of leaving groups to form stable cations.

Some considerations relating to the energies of the whole chemical process are presented schematically in Fig. 1. As the final product has an energy that lies 70 kcal mol^{-1} above that of the reactants, one would expect, without a knowledge of the electrochemical data, that dimerization leading to benzidine would hardly take place. Note, however, that the electrochemical evidence for this process comes from data obtained in solution. As is already known, the solvent influences the reaction profiles in two different ways: *i.e.* specifically and non-specifically.[39] Our results, which include one water molecule, take some account of the specific solvation for these reactions. However, given the different sizes of the initial and final radical cations, the non-specific solvent effect would clearly lower the energy of the products with respect to that of the reactants, therefore it has not been considered here. Nevertheless, as the non-specific solvent effect is expected to be quite similar for the different aromatic amines we have dealt with, we believe that its introduction will not affect the above-mentioned conclusions.

With regard to the oxidative dimerization of aromatic amines in the gas phase, if the water molecules solvating the leaving hydrogens are not included in the different stages of the dimerization of aniline presented in Fig. 1, because of the high energy of a lone proton, the final energy of **III** (benzidine plus two protons) will be more than 400 kcal mol^{-1} higher than that of the reactants. Therefore, this mechanism will not be operative. However, in this case it is conceivable that once the dicationic dimer is formed the two protons can undergo two 1,3-H shifts from the initial *para* carbon successively to the *ortho* carbon and the nitrogen so that the final product would not be benzidine but diprotonated benzidine. This mechanism is, at first sight, confirmed by exploratory thermodynamic AM1 calculations, which have shown that both dicationic dimers exist and are of increasing stability, so that diprotonated benzidine lies 6.6 kcal mol^{-1} below the energy of the initial two aniline radical cations. However, as to our knowledge, no experimental data have been reported for reactions of this kind in the gas phase no further work devoted to this point has been undertaken.

References

1 C. J. Schlesener, C. Amatore and J. K. Kochi, *J. Am. Chem. Soc.*, 1984, **106**, 7472.
2 R. S. Baumberger and V. D. Parker, *Acta Chem. Scand., Ser. B*, 1980, **34**, 537.
3 G. J. Kavarnos and N. J. Turro, *Chem. Rev.*, 1986, **86**, 401.
4 E. T. Seo, R. F. Nelson, J. M. Fritsch, L. S. Marcoux, D. W. Leedy and R. N. Adams, *J. Am. Chem. Soc.*, 1966, **88**, 3498.
5 R. F. Nelson and R. N. Adams, *J. Am. Chem. Soc.*, 1968, **90**, 3925.
6 R. I. Walter, *J. Am. Chem. Soc.*, 1966, **88**, 1923.
7 E. Steckhan, *Top. Curr. Chem.*, 1987, **142**, 1.
8 J. P. Dinnocenzo and T. E. Banach, *J. Am. Chem. Soc.*, 1989, **111**, 8646.
9 R. N. Adams, *Acc. Chem. Res.*, 1969, **2**, 175.
10 A. Vallat and E. Laviron, *J. Electroanal. Chem.*, 1970, **26**, 147.
11 D. Larumbe, I. Gallardo and C. P. Andrieux, *J. Electroanal. Chem.*, accepted.
12 A. R. Battersby, S. G. Hartley and D. M. Turnbull, *Tetrahedron Lett.*, 1978, 3169.
13 J. P. Collman, J. I. Brauman, K. M. Doxsee, T. R. Halbert, E. Bunnenberg, R. E. Linder, G. N. Lamor, J. Del Gaudio, G. Lang and K. Spartalian, *J. Am. Chem. Soc.*, 1980, **102**, 4182.
14 J. P. Collman, J. I. Brauman, K. M. Doxsee, J. L. Sessler, R. M. Morris and Q. H. Gibson, *Inorg. Chem.*, 1983, **22**, 1427.
15 M. Momenteau, J. Mispelter, B. Loock and J. M. Lhoste, *J. Chem. Soc., Perkin Trans. 1*, 1985, 221.
16 R. Young and C. K. Chang, *J. Am. Chem. Soc.*, 1985, **107**, 898.
17 D. B. Adams, *J. Chem. Soc., Perkin Trans. 2*, 1987, 247.
18 L. K. Vinson and J. J. Dannenberg, *J. Am. Chem. Soc.*, 1987, **111**, 2777.
19 M. J. S. Dewar, E. G. Zoebisch, E. G. Healy and J. J. P. Stewart, *J. Am. Chem. Soc.*, 1985, **107**, 3902.
20 M. J. S. Dewar and E. G. Zoebisch, *J. Mol. Struct., (Theochem)*, 1988, **40**, 1.
21 T. Sotomatsu, Y. Murata and T. Fujita, *J. Comput. Chem.*, 1989, **10**, 94.
22 J. J. Dannenberg, L. K. Vinson, M. Moreno and J. Bertran, *J. Org. Chem.*, 1989, **54**, 5487.
23 M. J. S. Dewar and Y. C. Yuan, *J. Am. Chem. Soc.*, 1990, **112**, 2088.
24 D. M. Camaioni, *J. Am. Chem. Soc.*, 1990, **112**, 9475.
25 J. A. Pople and R. K. Nesbet, *J. Chem. Phys.*, 1974, **22**, 571.
26 R. J. Duchovic, W. L. Hase and H. B. Schlegel, *J. Phys. Chem.*, 1984, **88**, 1339.
27 M. N. Paddon-Row and J. A. Pople, *J. Phys. Chem.*, 1985, **89**, 2768.
28 K. N. Houk, M. N. Paddon-Row, D. C. Spellmeyer, N. G. Rondan and S. Nagase, *J. Org. Chem.*, 1986, **51**, 2874.
29 T. Clark, in *A Handbook of Computational Chemistry*, Wiley-Interscience, New York, 1985.
30 R. Fletcher and M. D. Powell, *Comput. J.*, 1963, **6**, 163; W. C. Davidon, *Comput. J.*, 1968, **10**, 406.
31 J. W. McIver and A. Komornicki, *J. Am. Chem. Soc.*, 1972, **94**, 2625.

32 J. J. P. Stewart, *QCPE Bull.*, 1986, **6**, 91; QCPE program 455, version 3.1.
33 M. J. S. Dewar and J. J. P. Stewart, *QCPE Bull.*, 1986, **6**, 24; QCPE program 506.
34 S. Torii, in *Electroorganic Syntheses. Methods and Applications. Part I. Oxidations*, VCH, Weinheim, 1985, ch. 5, p. 153.
35 J. J. Dannenberg and L. K. Vinson, *J. Phys. Chem.*, 1988, **92**, 5635.
36 J. J. Dannenberg, *J. Phys. Chem.*, 1988, **92**, 6869.
37 S. Galera, J. M. Lluch, A. Oliva and J. Bertran, *J. Mol. Struct.*, (*Theochem.*), 1988, **40**, 101.
38 M. Moreno, I. Gallardo and J. Bertran, *J. Chem. Soc., Perkin Trans. 2*, 1989, 2017.
39 J. Bertran, in *New Theoretical Concepts for Understanding Organic Reactions*, eds. J. Bertran and I. G. Csizmadia, Kluwer, Dordrecht, 1989, p. 231.

Paper 1/00889G
Received 25*th February* 1991
Accepted 13*th May* 1991